





Summer Student Program

Characterisation Of The High Granularity Timing Detector Sensors

Author
Ramy Harib

Supervised by
Chiara Rizzi
Emma Kuwertz

September 25, 2019

Contents

Abstract **2**

1 introduction **2**

2 Sensors Test **5**

3 Results **6**
3.1 single pad sensors 6
3.2 2x2 sensors 7
3.2.1 HPK-Type1.1 7
3.2.2 HPK-Type1.2 10
3.2.3 HPK-Type2 12
3.2.4 HPK-Type3.1 15

4 Summary & Conclusion **17**

Appendices **19**

A List of 2x2 sensors **19**
A.1 HPK-TYPE1.1 19
A.2 HPK-TYPE1.2 20
A.3 HPK-TYPE2-2X2 20
A.4 HPK-TYPE3.1-2X2 21

Abstract

The High Granularity Timing Detector is a new piece of the ATLAS detector, which is going to be used for the high luminosity phase (phase II) of the large hadron collider (LHC), scheduled for 2026. In this project, we are studying the I-V characteristics of the sensors used for this detector using single pad probe station to make the measurements on single and 2x2 pad sensors.

1 introduction

ATLAS[1] Is a general-purpose experiment run by international collaboration at one of four collisions points at the Large Hadron Collider at CERN, its used to test the predictions of the standard model and beyond. Huge discovery was made until now and the most important one was the discovery of the Higgs Boson.

Atlas is considered to be the largest detector ever built, its 46m long, 25m in diameter, and it is located in a cavern 100m underground. It consists of four major components (see figure 1)

- **Inner tracker**: measures the direction, momentum, and charge of electrically charged particles produced in each proton-proton collision.
- **Calorimeters**: measures the energy of the produced particles by absorbing them.
- **Muon Spectrometer**: since muons can pass through the other detectors this detector is specialized in measuring the muons momenta
- **Magnet system**: used to bend the path of the charged particles to make it easier to contain their tracks.

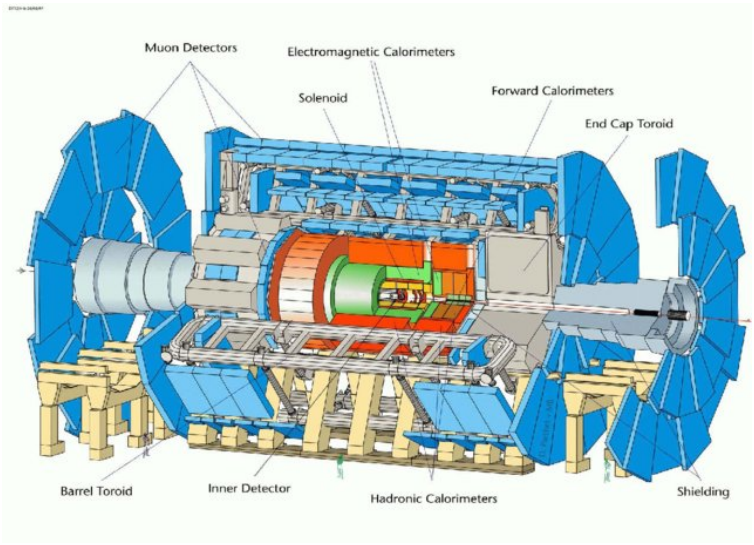


Figure 1: The ATLAS detector and its components [1]

ATLAS Phase-II upgrade (High luminosity phase)[2]: It's planned to increase the instantaneous luminosity to 7.5 x 1034 cm^{-2} s^{-1} in 2026, which is an increase by a factor of approximately five compared to the luminosities of Run 2. Higher luminosity means higher number of events that is due to the increase of the collision rate, which leads to increase in the probability to observe more rare processes.

Significant upgrades of the ATLAS detector will take place in order to withstand the high-radiation environment and to reduce the effects of the pileup. A High-Granularity Timing Detector (see figure 2) is used to distinguish between collisions occurring very close in space but separated in time. It composes of four layers of low gain avalanche diodes, the sensors are designed to provide a fast signal in response to charged particles for a time resolution per hit of 40 ps at the start and 70 - 85 ps at the end of lifetime. The charge should be at least 2.5 fC and the hit efficiency at least 95%. The granularity should be 1.3mm x 1.3mm and the physical thickness below 300 μm. The sensor should be of total active size of 39mm x 19.5mm with 30 x 15 pads. The maximum leakage current should be less than 5 μA per pad and the applied bias voltage less than 750V.[3]

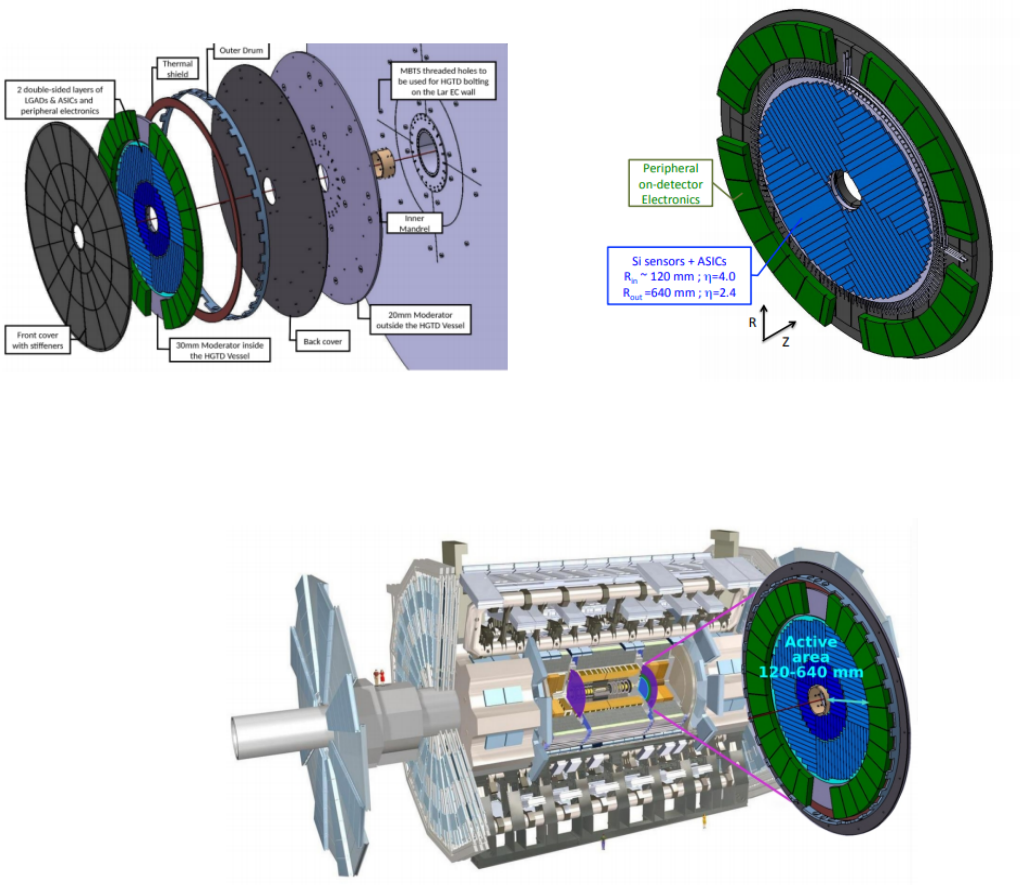
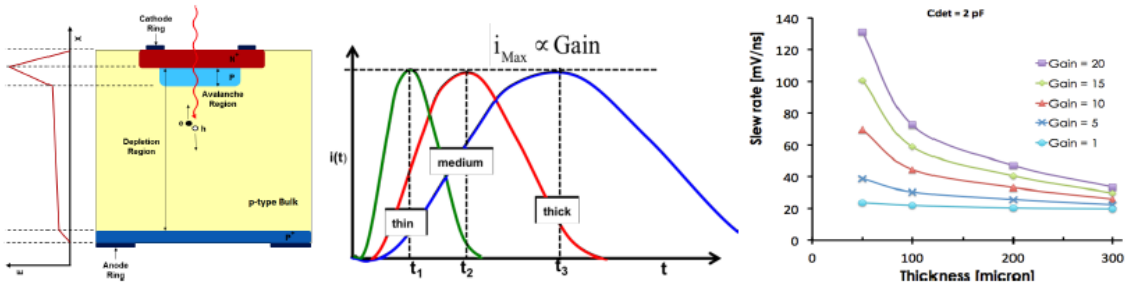


Figure 2: Illustration of the HGTD, and it's position in ATLAS .The blue represents the active region and the green the off detector electronic.[1]

[1]The ATLAS High Granularity Timing Detector by Sacerdoti, Sabrina

Silicon Low Gain Avalanche Detector (LGAD) is the technology used for the HGTD sensors. It is based on the PiN diode structure and it consists of N-P junction over highly doped p-type (p+), this will creat a high electric field region Figure 3(a). It is operated in high reversed bias voltage to get as wide depletion region as possible. Whenever a charged particle passes through the detector, an electron hole pair is created in the depletion region, which causes to generate a large current by drifting of the holes to the p+ region. Standard PiN diodes are seriously affected by thermal and electronic noise. Moreover, Exposing them to high irradiation causes irrecoverable damage (Acceptors removal) and decrease in signal-to-noise ratio.
LGAD provide a moderate multiplication (gain ≈ 20) on the collected charge, which leads to a significant increase in the signal to noise ratio.[4]

The signal height iMax of the LGAD is proportional to the gain M, it is independent of the detector thickness as illustrated in Figure 3(b). Figure 3(c) shows that the signal slope dV/dt depends on the thickness of the sensor.



(a) Cross section of an LGAD diode.

(b) Current signals for LGADs of different thicknesses.

(c) Signal slope as function of LGAD thickness.

Figure 3: Working principle of the LGAD sensors and how their response depends on sensor thickness[3].

The two major effects determine the time resolution are the time walk and the time jitter. Both depend inversely on the signal slope dV/dt:

$$\sigma_{TimeWalk} = \left(\frac{V_{th}}{\frac{S}{t_{rise}}} \right)_{RMS} \propto \left(\frac{N}{\frac{dV}{dt}} \right)_{RMS} \tag{1}$$

$$\sigma_{Jitter} = \frac{N}{dV/dt} \approx \frac{t_{rise}}{S/N} \tag{2}$$

where S refers to the signal, N to the noise, t_{rise} to the rise time, and V_{th} to the threshold voltage.The best time resolution is achieved with thin sensor and large gain.[3]

2 Sensors Test

Electrical measurements (I-V characteristic) has been done in this project for various types of sensors to examine their breakdown voltage and leakage current. We want to compare between the behaviour of the single pad and the 2x2 pads sensors. Eventually to decide which type would be most appropriate for the next upgrade.

The measuring setup used consists of a keithley 2410 which is the power supply, and a keithley 6487 is the Ammeter used to measure the pad current (see figure 4). Both of the Keithleys are connected to a cabinet that has a chuck inside that is connected to the power supply, a microscope to enable placing the sensor in the right position on the chuck, and a three connection needles that can be adjusted precisely to place them on the exact position.

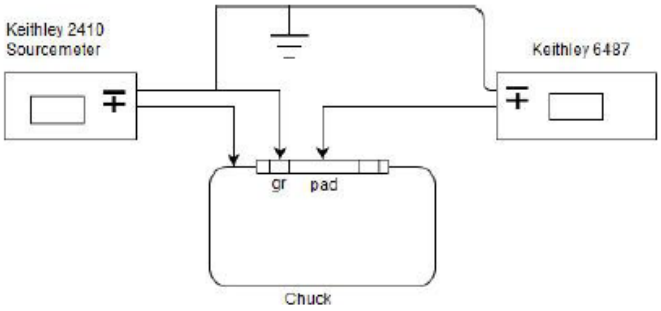


Figure 4: schematic diagram of the probe station[2]

Reverse bias is applied by the Keithley 2410 sourcemeter to the sensor through the chuck. The guard ring is connected to ground. The pad of the sensor is connected to the Keithley 6487 Ammeter. An actual example connection is shown in Figure 5. The circle in the middle is the pad, the ground is connected to one of the rectangles on the edges. A vacuum is utilized to fix the sensorâs position.

Using LabVIEW to control the measurements. We set the maximum applied voltage, number increment steps, and the compliance current to avoid damaging of the sensor due to the very high current at breakdown.
2x2s sensors consist of four pads compact together and they are connected the same way as the single ones (see Figure 6). We measure one pad at a time and keeping the others floating. By keeping the neighbouring pads floating, we cannot know their impact on the measurements.

[2]drwan by Afonso Soares Canas Ferreira

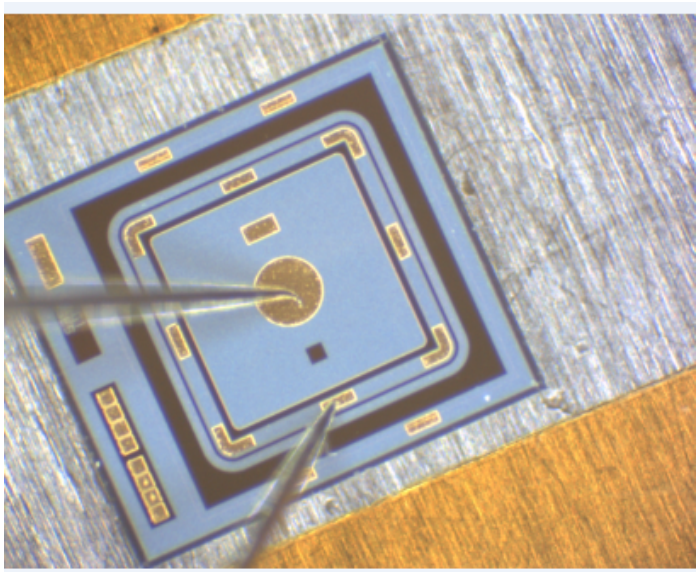


Figure 5: photo of single pad HPK-Type-1.1-LG1-SE5-2 sensor

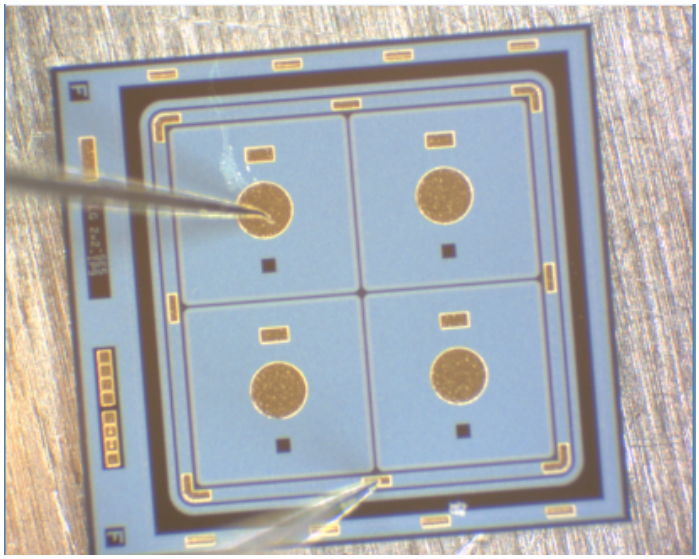


Figure 6: photo of the HPK-TYPE3-1-LG-2X2-SE5-2-IP3-W3

3 Results

During this project, the sensors measured were the single pad of the HPK type 1.1, 1.2, 2, and 3.1 .Also the 2x2s were measured from the same type of the single ones but type 3.2 instead of type 3.1 was measured.

3.1 single pad sensors

Figure 7 shows a summary of all the single pad sensors measured. Total current is the current supplied by the source, Pad current is the sensor's leakage current, and Guard ring current comes from the surface leakage current, which is the difference between the total and the pad current. Each type had different breakdown voltage and different leakage current. However, sensors from the same type had almost the same curves. Type 1.1 of the both configurations (SE5 and SE3) brokedown at 218V,

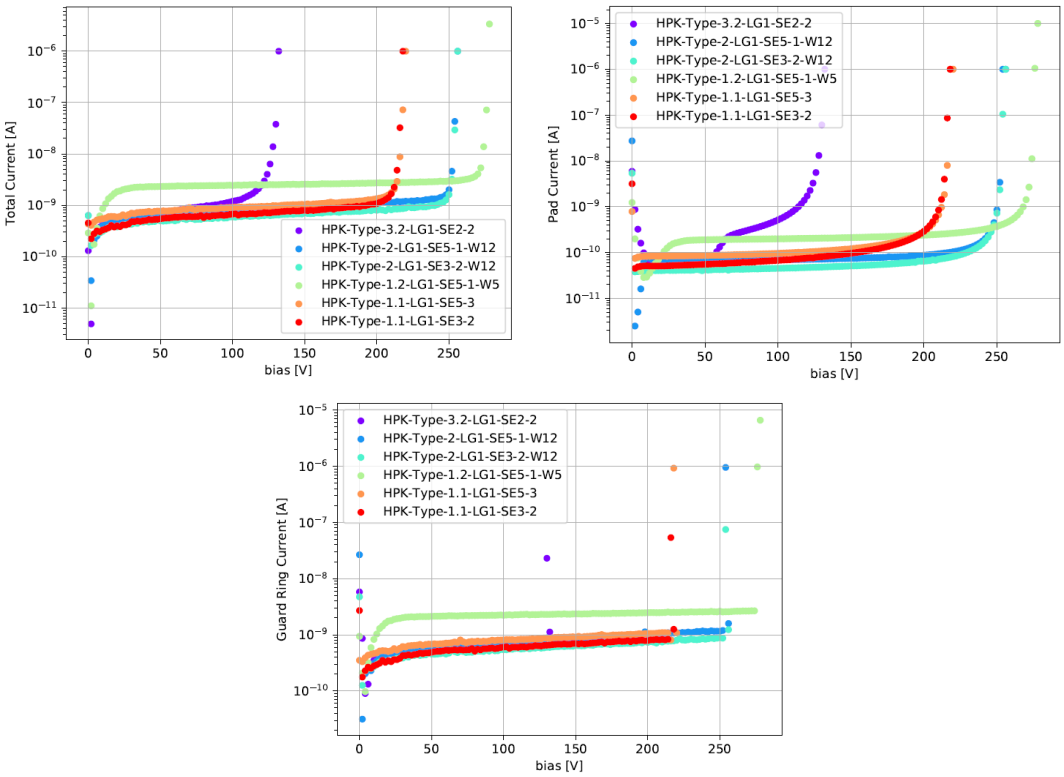


Figure 7: Current as a function of bias voltage for HPK single pad sensors. Shown are the total current (top left), pad current (top right) and guard ring current (bottom).[3]

Type 1.2 brokedown at 278V, Type 2 of the both configurations brokedown at 256, and finally type 3.2 brokedown at 132V.The leakage current (total) was an order of a few Nano amps.

3.2 2x2 sensors

The following plots (figures 8-23) show summary of every type measured, sensors had odd characteristic, example of a consistent results, and the PiN diodes of each type.

3.2.1 HPK-Type1.1

Figure 8 shows the characteristic of the type 1.1 sensors. The breakdown voltage was at 215V for almost all of the sensors, and the leakage current was in order of a few Nano Amps. However, we had outliers in one of the sensors, three of its pads had early breakdown at 120V and the fourth one brokedown immediately! (See figure 9).An example of appropriate results is illustrated in figure 10. In figure 11 the characteristic of the PiN diode of this type is shown. Although one of the pads had strange behaviour before breakdown, they all brokedown at 400V.

[3]HPK is the manufacturer company (Hamamatsu Photonics),Type3.1 refers to the sensor type,LG for Low Gain or sometimes PIN is used instead for PIN diode, 2x2 for the number of pads in the sensor,SE5 is the pads configuration used, 2 used for numbering the identical sensors, IP3 for the gap width between neighbouring pads on an array , W3 is the wafer number and the position of the pads will be labeled as 00, 01, 10, and 11 for top left, top right, bottom left, and bottom right respectively.

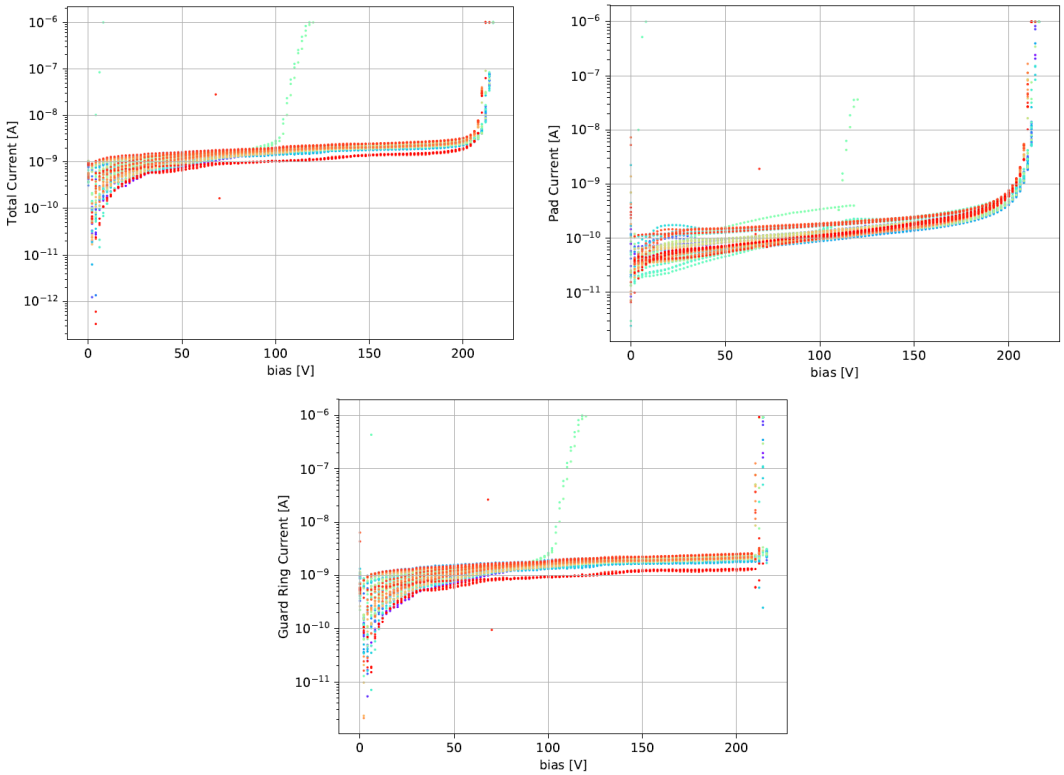


Figure 8: Current as a function of bias voltage for HPK-type1.1-2x2 sensors (curve per pad). Shown are the total current (top left), pad current (top right) and guard ring current (bottom).

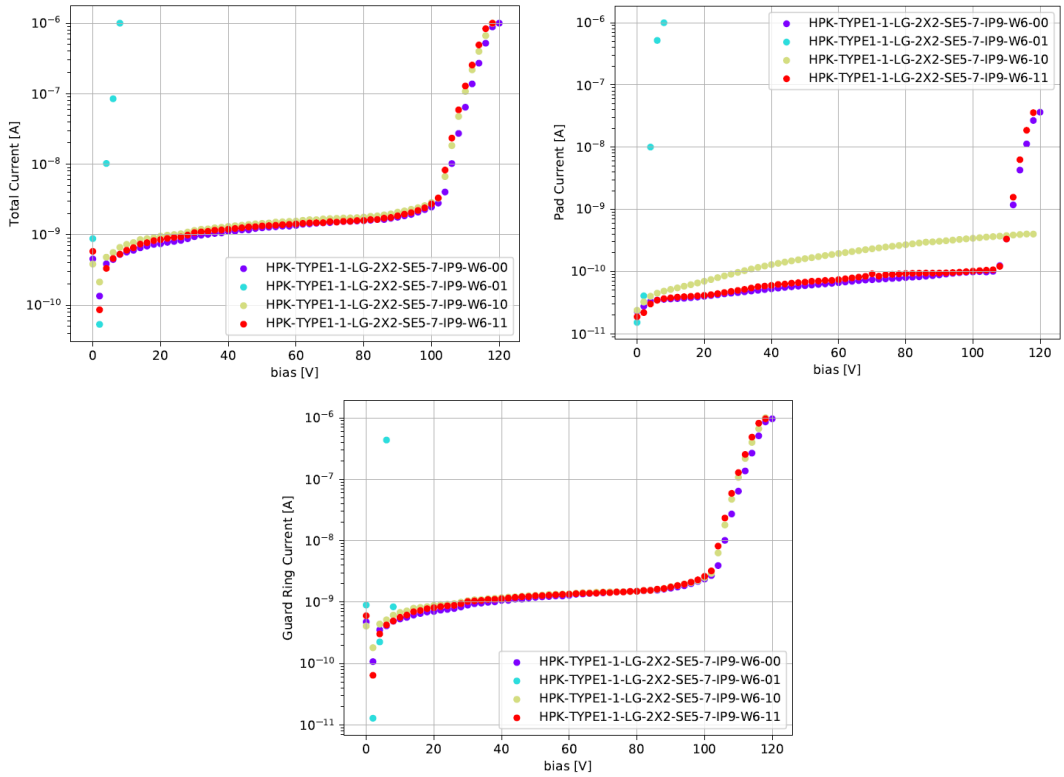


Figure 9: Current as a function of bias voltage for HPK-TYPE1-1-LG-2X2-SE5-7-IP9-W6, which had earlier breakdown than expected. Shown are the total current (top left), pad current (top right) and guard ring current (bottom).

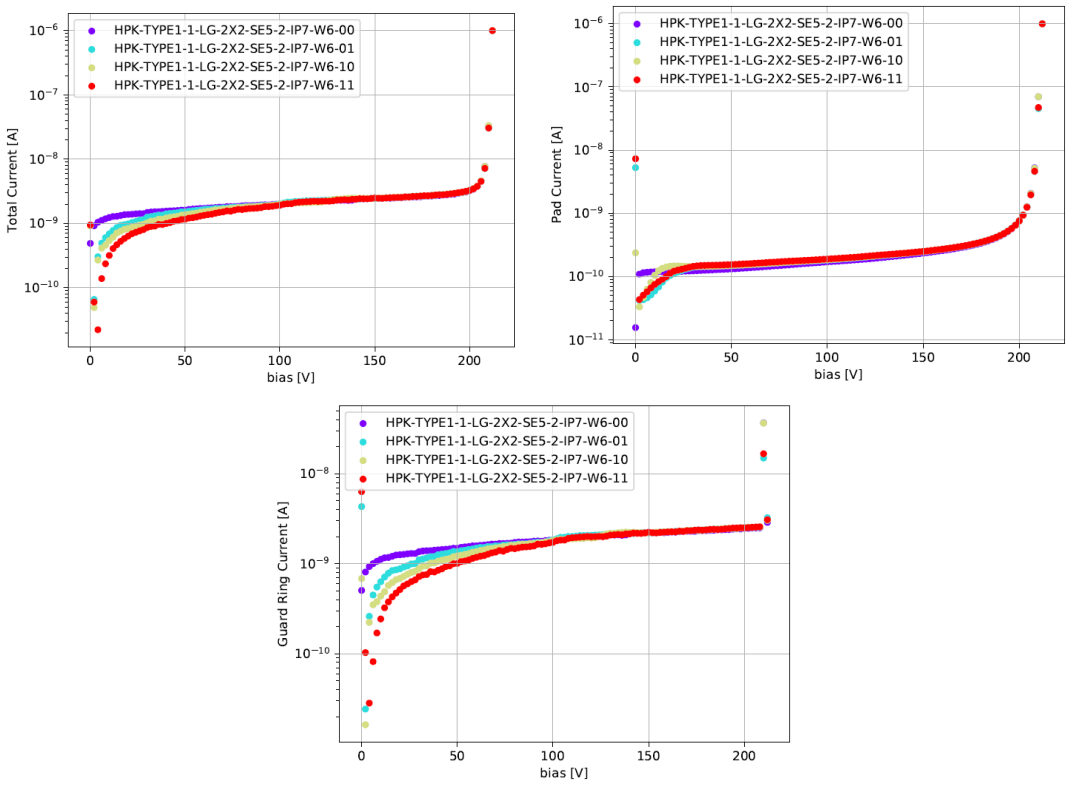


Figure 10: Current as a function of bias voltage for HPK-TYPE1-1-LG-2X2-SE5-2-IP7-W6. Shown are the total current (top left), pad current (top right) and guard ring current (bottom).

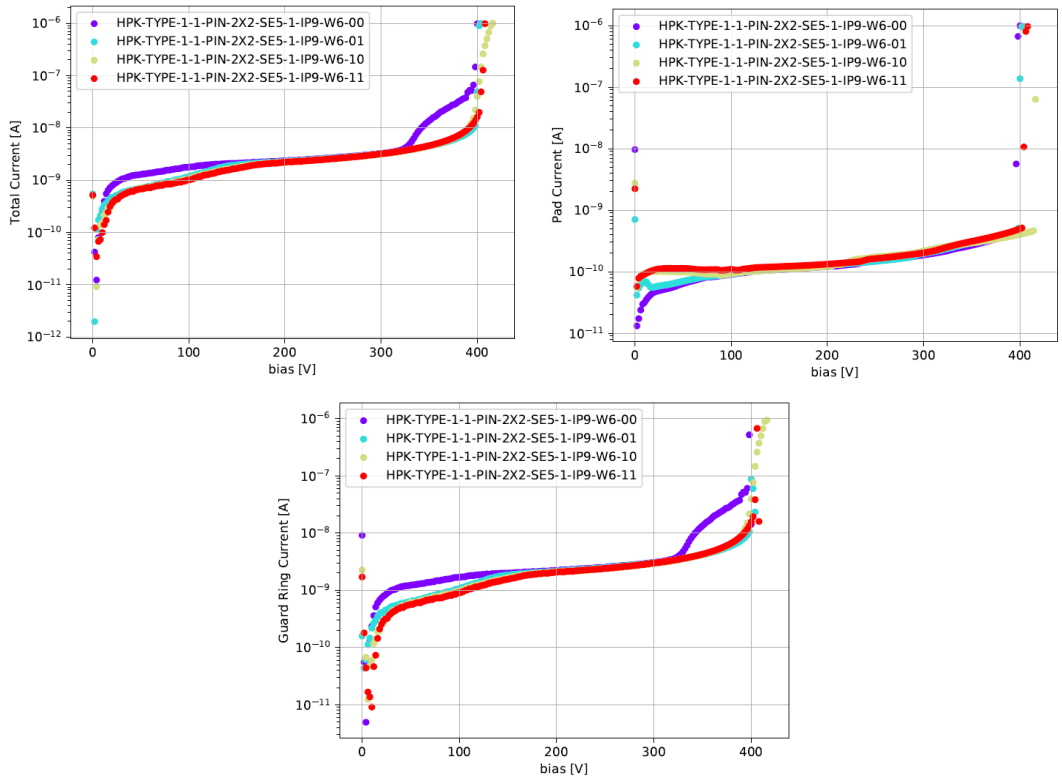


Figure 11: Current as a function of bias voltage for HPK-TYPE-1-1-PIN-2X2-SE5-1-IP9-W6. Shown are the total current (top left), pad current (top right) and guard ring current (bottom).

3.2.2 HPK-Type1.2

[h!] Figure 12 shows the characteristic of the type 1.2 sensors. The breakdown voltage was in the range of (265V-280 v).But for a single sensor all the pads had the same value (see figure 14).The leakage current was about 10 Nano Amps. One of the sensors had strange shape and it brokedown very late (about 300V) as shown in figure 13.In figure 15 the characteristic of the PiN diode of this type is shown, it had a breakdown at 580V.

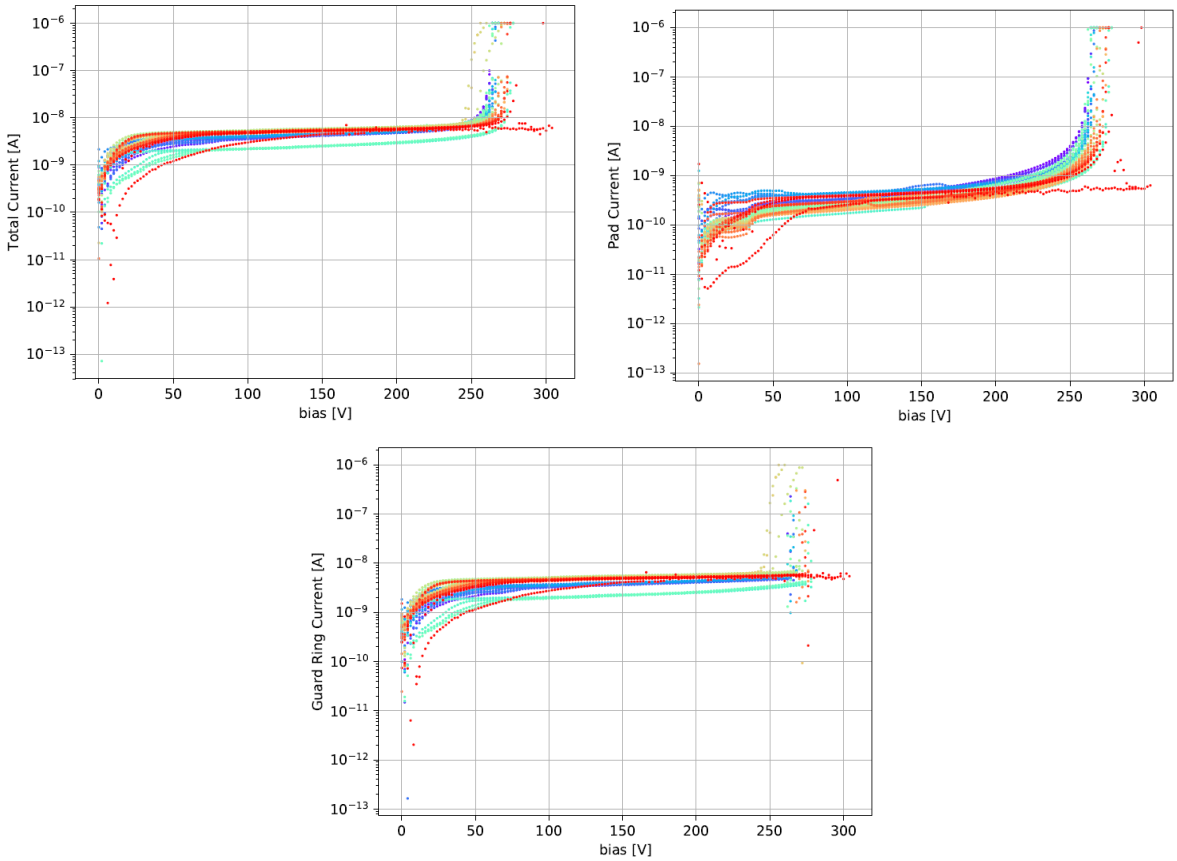


Figure 12: Current as a function of bias voltage for HPK-type1.2 2x2 sensors (curve per pad). Shown are the total current (top left), pad current (top right) and guard ring current (bottom).

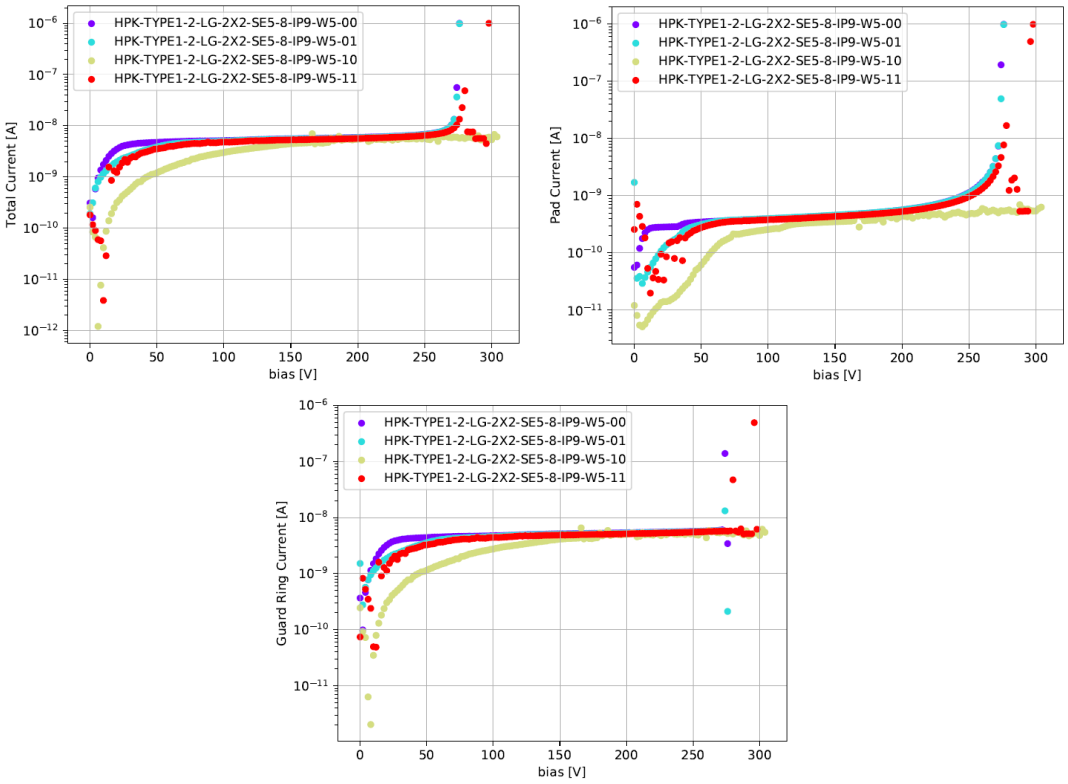


Figure 13: Current as a function of bias voltage for HPK-TYPE1-2-LG-2X2-SE5-8-IP9-W5 measurements, which had late breakdown. Shown are the total current (top left), pad current (top right) and guard ring current (bottom).

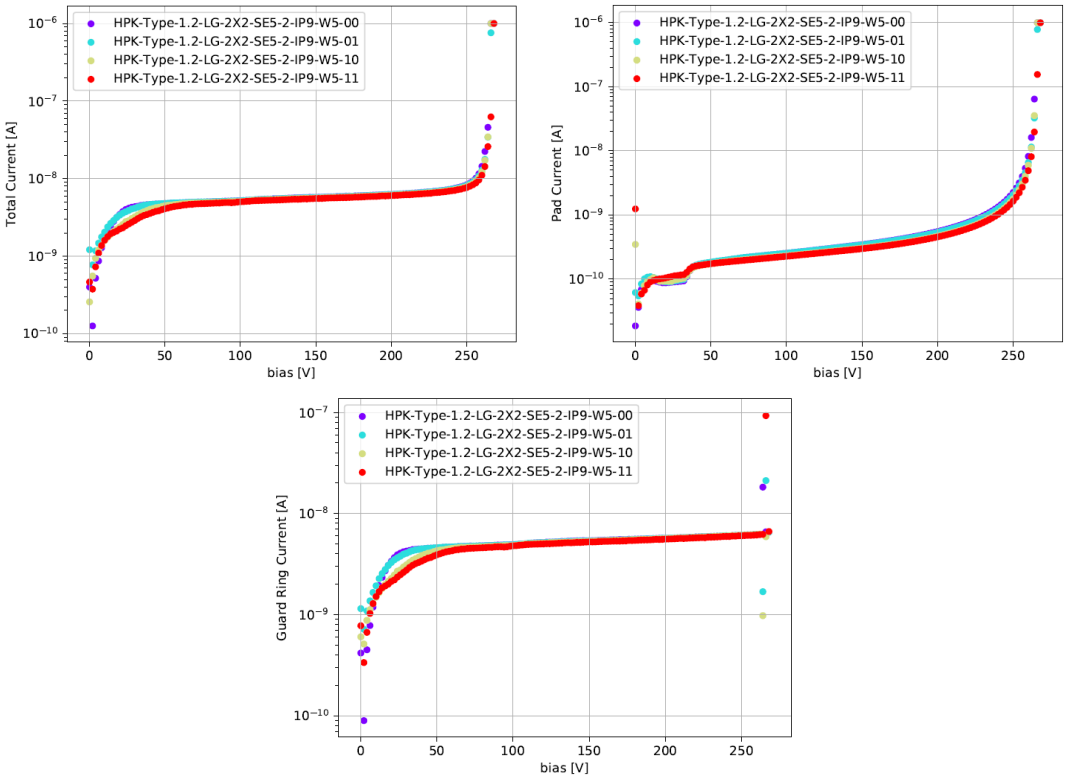


Figure 14: Current as a function of bias voltage for HPK-Type-1.2-LG-2X2-SE5-2-IP9-W5. Shown are the total current (top left), pad current (top right) and guard ring current (bottom).

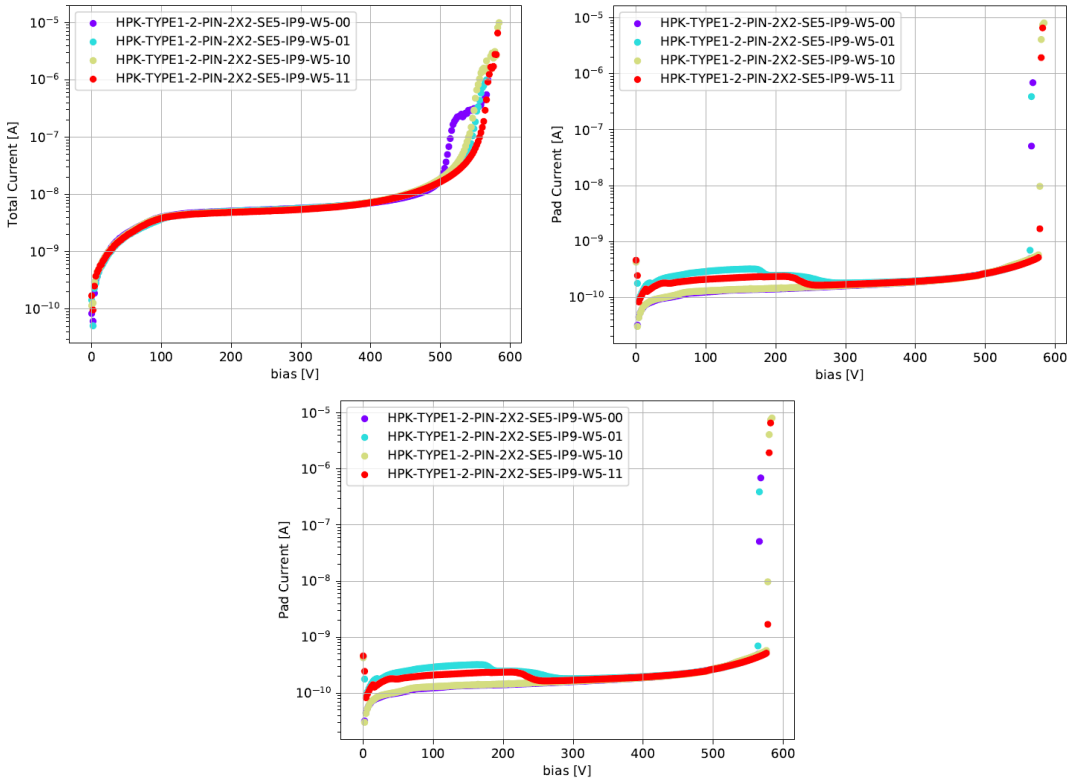


Figure 15: Current as a function of bias voltage for HPK-TYPE1-2-PIN-2X2-SE5-IP9-W5. Shown are the total current (top left), pad current (top right) and guard ring current (bottom).

3.2.3 HPK-Type2

Figure 16 shows the characteristic of the type2 sensors. They had a VBD at 248V.an example of a consistent results is illustrated in 18.The leakage current was about few Nano Amps. There was a late breakdown in one of the pads (about 376V) and it had odd behaviour as shown in figure 17.In figure 19 the characteristic of the PiN diode of this type is shown. It brokedown at 390V.

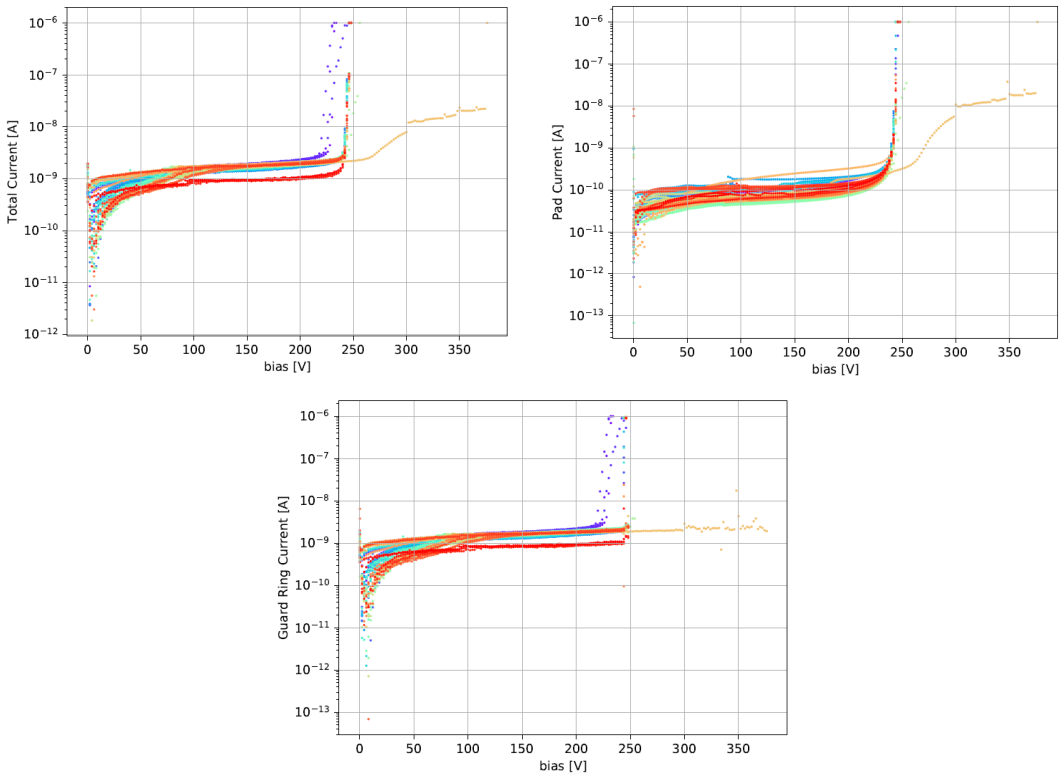


Figure 16: Current as a function of bias voltage for HPK-type2-2x2 sensors (curve per pad). Shown are the total current (top left), pad current (top right) and guard ring current (bottom).

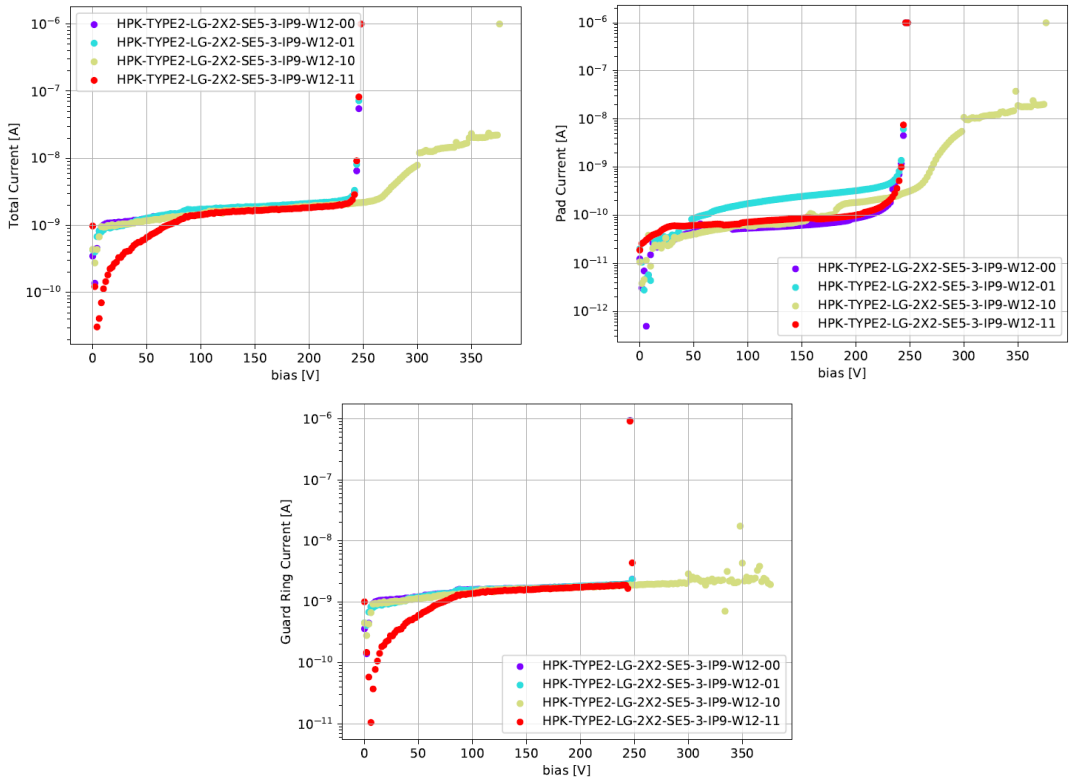


Figure 17: Current as a function of bias voltage for HPK-TYPE2-LG-2X2-SE5-3-IP9-W12, which had strange behaviour. Shown are the total current (top left), pad current (top right) and guard ring current (bottom).

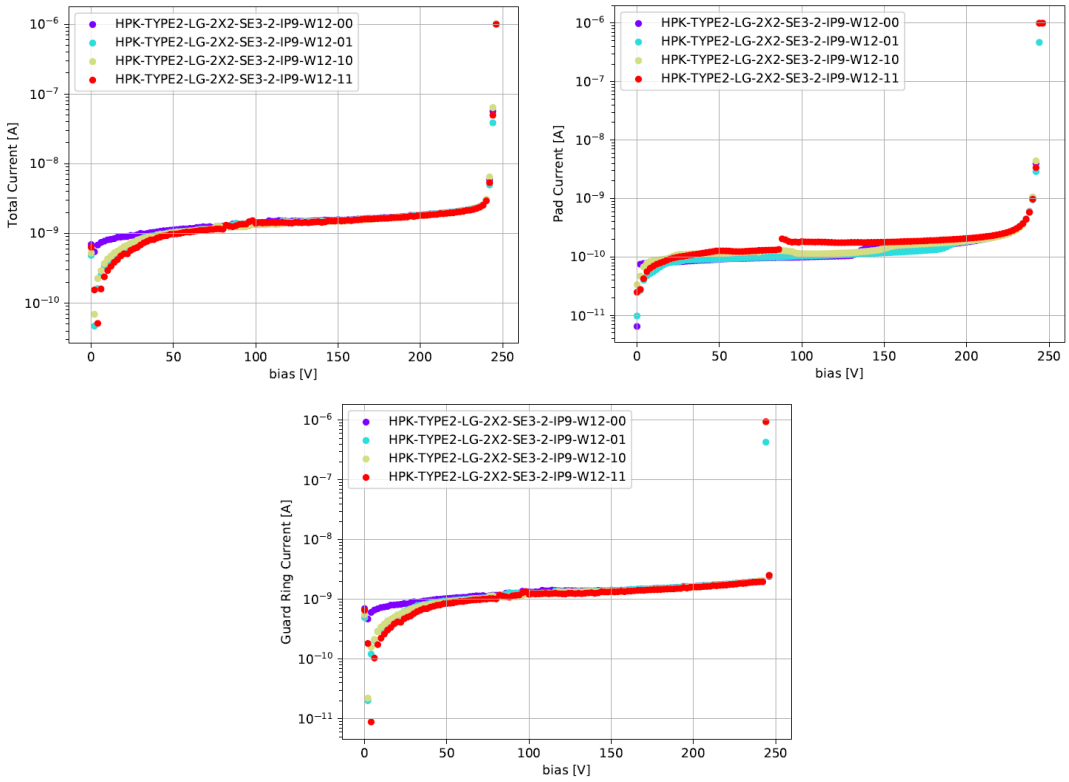


Figure 18: Current as a function of bias voltage for HPK-TYPE2-LG-2X2-SE3-2-IP9-W12, which had strange behaviour. Shown are the total current (top left), pad current (top right) and guard ring current (bottom).

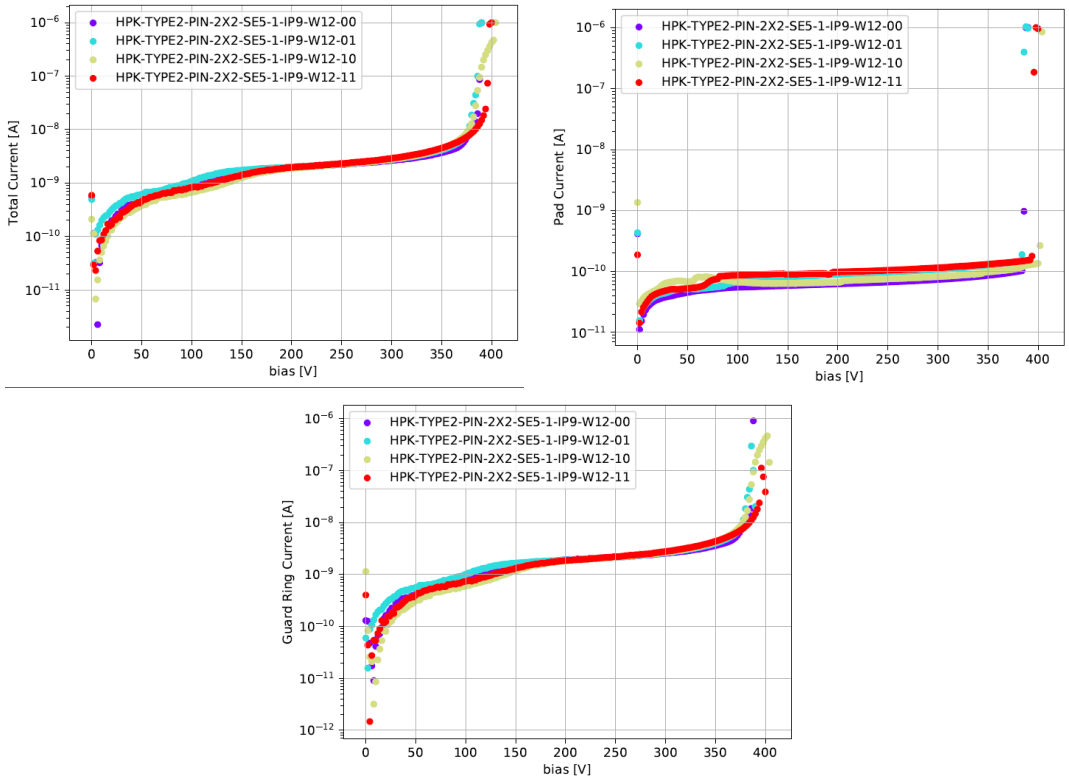


Figure 19: Current as a function of bias voltage for HPK-TYPE2-PIN-2X2-SE5-1-IP9-W12, which had strange behaviour. Shown are the total current (top left), pad current (top right) and guard ring current (bottom).

3.2.4 HPK-Type3.1

Figure 20 shows the characteristic of the type3.1 sensors. Their VBD was in the range of (231V-251V).But for the same sensor the four pads had similar values (see figure 22).The leakage current was about few Nano Amps. There was a late breakdown in one of the sensors and it had strange curve (see figure 21).In figure 23 the characteristic of the PiN diode of this type is shown they brokedown at different values.

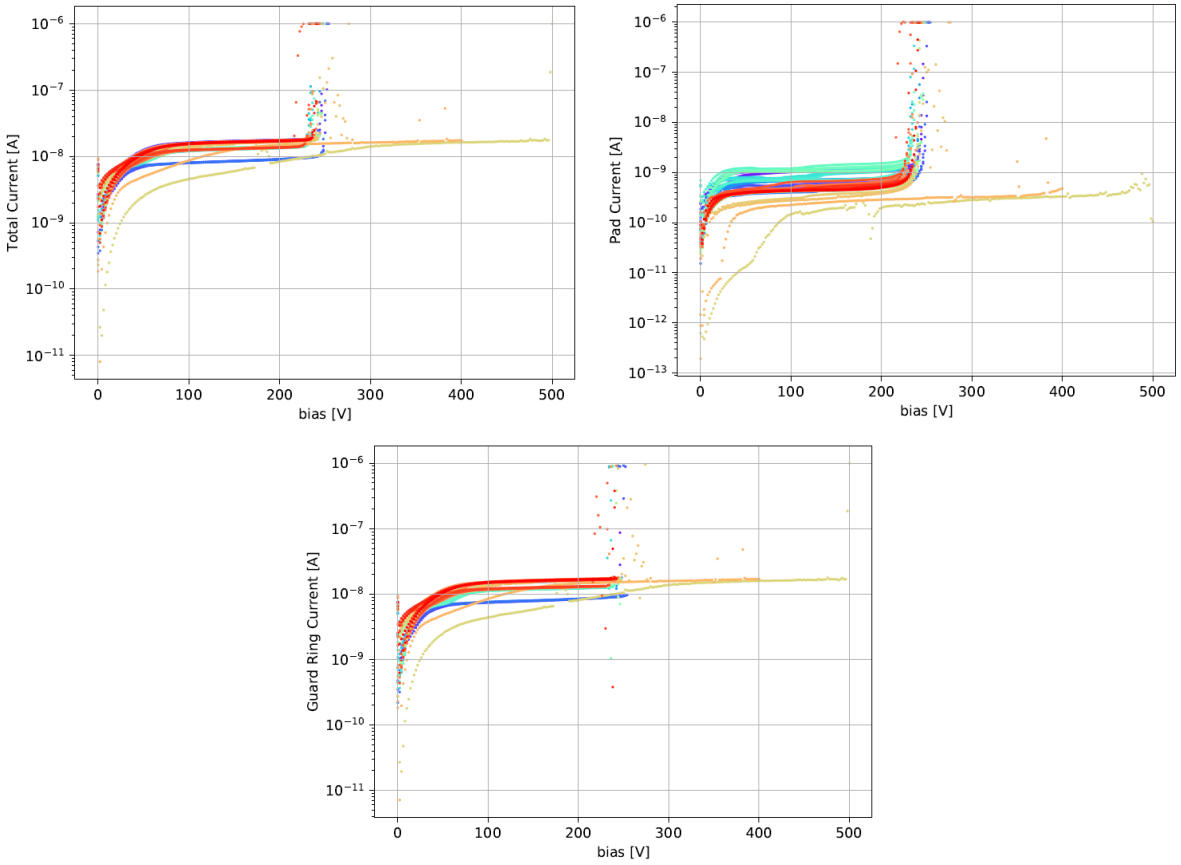


Figure 20: Current as a function of bias voltage for HPK-Type3.1-2x2 sensors (curve per pad). Shown are the total current (top left), pad current (top right) and guard ring current (bottom).

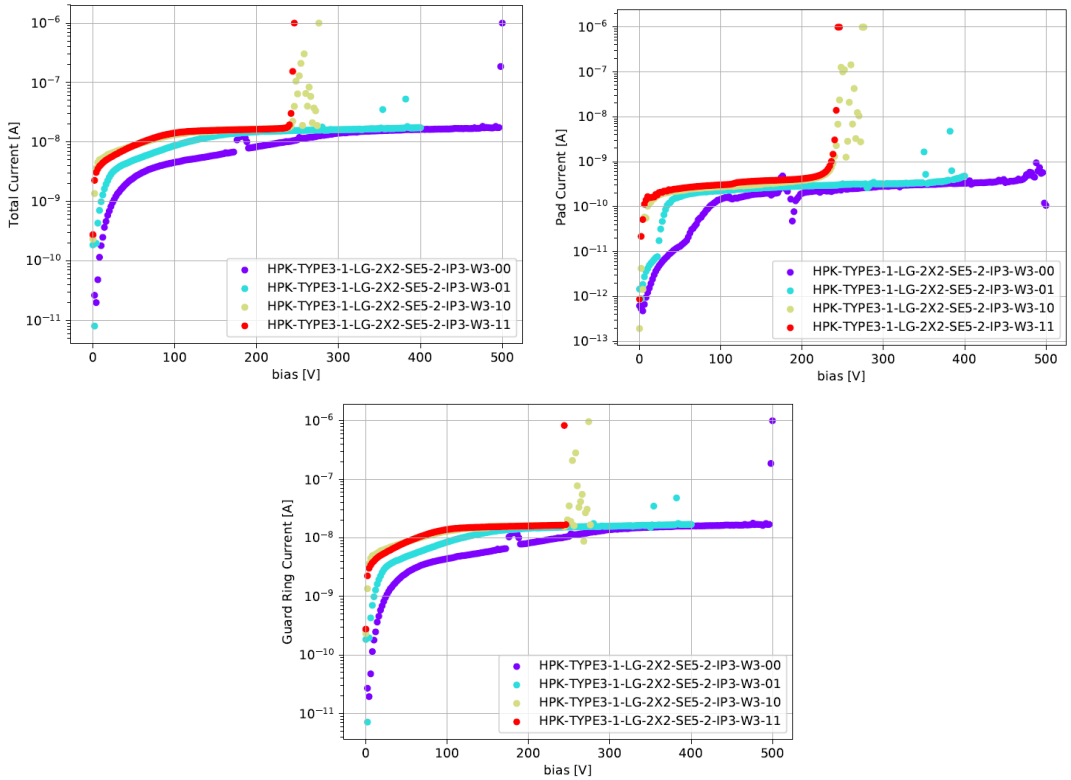


Figure 21: Current as a function of bias voltage for HPK-TYPE1-1-LG-2X2-SE5-7-IP9-W6, which had late breakdown (pad 00 and 01). Shown are the total current (top left), pad current (top right) and guard ring current (bottom).

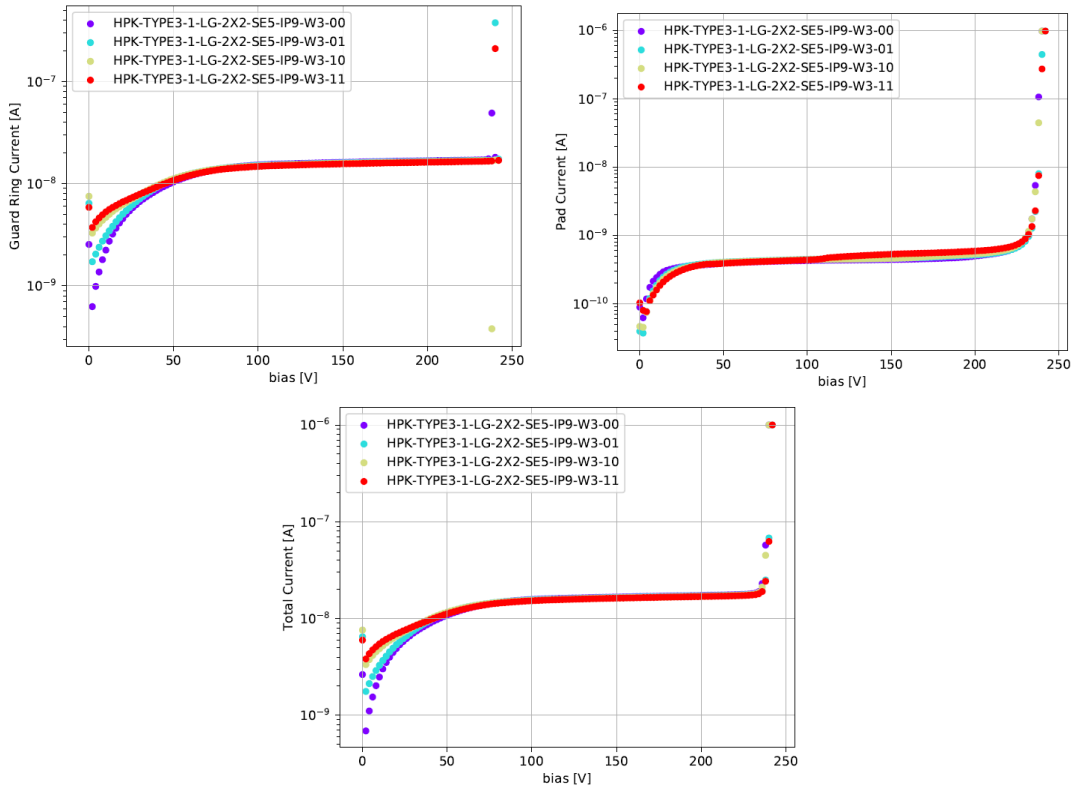


Figure 22: Current as a function of bias voltage for HPK-TYPE3-1-LG-2X2-SE5-IP9-W3. Shown are the total current (top left), pad current (top right) and guard ring current (bottom).

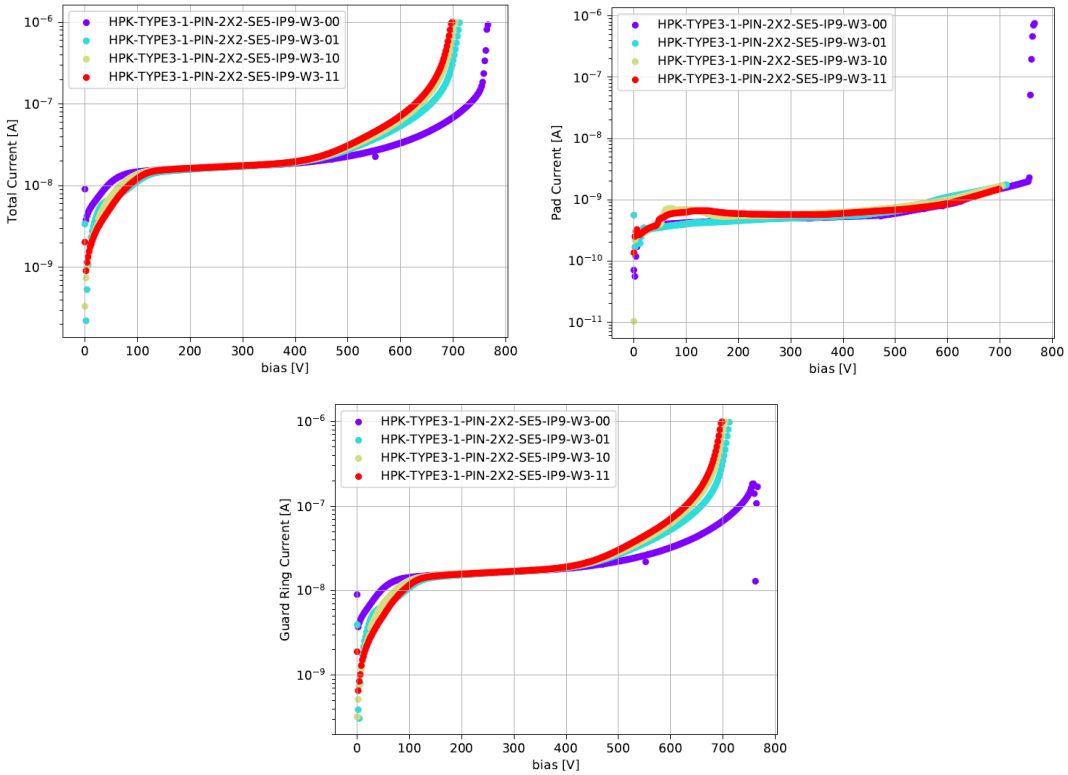


Figure 23: Current as a function of bias voltage for HPK-TYPE3-1-PIN-2X2-SE5-IP9-W3. Shown are the total current (top left), pad current (top right) and guard ring current (bottom).

4 Summary & Conclusion

A summary of the previous results is shown illustrated in Table 1

Sensor Type	VBD (V)	Leakage current (nA)
HPK-Type1.1	215	2
HPK-Type1.1-PIN	400	2
HPK-Type1.2	265-280	8
HPK-Type1.2-PIN	580	8
HPK-Type2	248	1-2
HPK-Type2-PIN	390	3
HPK-Type3.1	231-251	20
HPK-Type3.1-PIN	698-766	20

Table 1: summary of VBD and Leakage current for every sensor type.

Conclusion

In this project I made I-V measurements on some single pad sensors, and all of the 2x2 sensors that they were measured for the first time by the HGTD group .Although there was unpredicted results in some of the sensors (had early or late breakdown than expected), the measurements were confirmed by other institutes.

Next steps

- update the current setup for C-V measurements.
- measure the irradiated sensors.

References

[1] `https://atlas.cern`.

[2] "ATLAS Phase-II Upgrade Scoping Document," Tech. Rep. CERN-LHCC-2015-020. LHCC-G-166, CERN, Geneva, Sep 2015.

[3] A. Collaboration, "Technical Proposal: A High-Granularity Timing Detector for the ATLAS Phase-II Upgrade," Tech. Rep. CERN-LHCC-2018-023. LHCC-P-012, CERN, Geneva, Jun 2018.

[4] P. FernÃ¡ndez-MartÃnez, D. Flores, V. Greco, S. Hidalgo, G. Pellegrini, D. Quirion, M. FernÃ¡ndez-GarcÃa, I. Vila, and G. Kramberger, "Low gain avalanche detectors for high energy physics," in *2015 10th Spanish Conference on Electron Devices (CDE)*, pp. 1–4, Feb 2015.

Appendices

A List of 2x2 sensors

A.1 HPK-TYPE1.1

- HPK-type1.1-LG-2X2-SE2-1-IP9-W6.
- HPK-TYPE1-1-LG-2X2-SE3-1-IP7-W6.
- HPK-TYPE1-1-LG-2X2-SE3-2-IP7-W6.
- HPK-TYPE1-1-LG-2X2-SE5-1-IP9-NM-W6
- HPK-TYPE1-1-LG-2X2-SE5-2-IP7-W6
- HPK-TYPE1-1-LG-2X2-SE5-3-IP9-W6
- HPK-TYPE1-1-LG-2X2-SE5-4-IP9-W6
- HPK-TYPE1-1-LG-2X2-SE5-5-IP9-W6
- HPK-TYPE1-1-LG-2X2-SE5-6-IP9-W6
- HPK-TYPE1-1-LG-2X2-SE5-7-IP9-W6
- HPK-TYPE1-1-LG-2X2-SE5-8-IP3-W6
- HPK-TYPE1-1-LG-2X2-SE5-9-IP9-UBM-W6
- HPK-TYPE-1-1-PIN-2X2-SE5-1-IP9-W6

A.2 HPK-TYPE1.2

- HPK-Type-1.2-LG-2X2-SE3-1-IP9-W5
- HPK-Type-1.2-LG-2X2-SE3-2-IP5-W5
- HPK-Type-1.2-LG-2X2-SE3-3-IP7-W5
- HPK-Type-1.2-LG-2X2-SE5-2-IP9-W5
- HPK-Type-1.2-LG-2X2-SE5-3-IP9-UBM-W5
- HPK-TYPE1-2-LG-2X2-SE2-1-IP9-W5
- HPK-TYPE1-2-LG-2X2-SE5-1-IP9-NM-W5
- HPK-TYPE1-2-LG-2X2-SE5-3-IP9-W5
- HPK-TYPE1-2-LG-2X2-SE5-4-IP9-W5
- HPK-TYPE1-2-LG-2X2-SE5-5-IP9-W5
- HPK-TYPE1-2-LG-2X2-SE5-6-IP3-W5
- HPK-TYPE1-2-LG-2X2-SE5-7-IP9-W5
- HPK-TYPE1-2-LG-2X2-SE5-8-IP9-W5
- HPK-TYPE1-2-PIN-2X2-SE5-IP9-W5

A.3 HPK-TYPE2-2X2

- HPK-TYPE2-LG-2X2-SE2-1-IP9-W12
- HPK-TYPE2-LG-2X2-SE3-1-IP9-W12
- HPK-TYPE2-LG-2X2-SE3-2-IP9-W12
- HPK-TYPE2-LG-2X2-SE3-3-IP9-W12
- HPK-TYPE2-LG-2X2-SE5-1-IP7-W12
- HPK-TYPE2-LG-2X2-SE5-2-IP9-W12
- HPK-TYPE2-LG-2X2-SE5-3-IP9-W12
- HPK-TYPE2-LG-2X2-SE5-4-IP9-W12
- HPK-TYPE2-LG-2X2-SE5-5-IP9-W12
- HPK-TYPE2-LG-2X2-SE5-6-IP3-W12
- HPK-TYPE2-LG-2X2-SE5-7-IP9-UBM-W12
- HPK-TYPE2-LG-2X2-SE5-8-IP9-W12
- HPK-TYPE2-LG-2X2-SE5-IP9-NM-W12
- HPK-TYPE2-PIN-2X2-SE5-1-IP9-W12

A.4 HPK-TYPE3.1-2X2

- HPK-TYPE3-1-LG-2X2-SE2-1-IP9-W3
- HPK-TYPE3-1-LG-2X2-SE3-1-IP9-W3
- HPK-TYPE3-1-LG-2X2-SE3-2-IP7-W3
- HPK-TYPE3-1-LG-2X2-SE3-3-IP5-W3
- HPK-TYPE3-1-LG-2X2-SE5-1-IP9-W3
- HPK-TYPE3-1-LG-2X2-SE5-2-IP3-W3
- HPK-TYPE3-1-LG-2X2-SE5-3-IP9-W3
- HPK-TYPE3-1-LG-2X2-SE5-4-IP9-W3
- HPK-TYPE3-1-LG-2X2-SE5-5-IP9-W3
- HPK-TYPE3-1-LG-2X2-SE5-6-IP9-W3
- HPK-TYPE3-1-LG-2X2-SE5-IP9-NM-W3
- HPK-TYPE3-1-LG-2X2-SE5-IP9-UBM
- HPK-TYPE3-1-LG-2X2-SE5-IP9-W3
- HPK-TYPE3-1-PIN-2X2-SE5-IP9-W3